

Effects of Heterogeneous Vibration Frequencies on Joint Coordination in Multi-DOF Upper-Limb Stimulation

Wenbin Liu^{1†}, Kazuo Kiguchi² and Yue Hou³

¹College of Information Science and Engineering, Ritsumeikan University, Osaka, Japan
(Tel: +81-70-1826-4059; E-mail: liu-wb@fc.ritsumeik.ac.jp)

²Department of Mechanical Engineering, Kyushu University, Fukuoka, Japan
(E-mail: kiguchi@ieee.org)

³Department of Mechanical Engineering, Kyushu University, Fukuoka, Japan
(E-mail: hou.yue.822@m.kyushu-u.ac.jp)

Abstract: Mechanical vibration delivered to muscle or tendon can evoke the tonic vibration reflex (TVR), a spinal response that generates involuntary muscle contraction without external actuation. Leveraging this mechanism, vibration-based stimulation offers a lightweight alternative for motor rehabilitation, particularly in patients who lack sufficient voluntary control. This study examines how joint-specific vibration frequencies—i.e., heterogeneous frequency combinations across muscles—affect multi-degree-of-freedom (multi-DOF) upper-limb motion driven solely by TVR. Vibration was applied to four muscles spanning the shoulder and elbow joints: posterior deltoid and pectoralis major (controlling shoulder horizontal adduction/abduction) and biceps and triceps brachii (controlling elbow flexion/extension). Experimental results show that differential stimulation frequencies significantly modulate joint-specific activation strength and inter-joint coordination, revealing frequency-dependent tuning characteristics of TVR in a multi-joint context. These findings provide a foundation for adaptive vibration-based rehabilitation systems that align assistance with individual neuromuscular needs while avoiding bulky robotic actuation.

Keywords: Mechanical vibration stimulation, tonic vibration reflex, Upper limb movement, rehabilitation strategy.

1. INTRODUCTION

Stroke remains one of the most prevalent motor disorders worldwide, and effective recovery generally requires prolonged, intensive rehabilitation to re-establish damaged neural circuits [1]. In response, a growing array of intelligent rehabilitation devices has been developed. Current solutions fall broadly into two categories: (i) exoskeleton or robot-arm systems that generate external forces to guide the patient's limb [2]-[6], and (ii) neuromuscular stimulation techniques (typically electrical) that provoke muscle contractions to produce movement [7][8]. More recently, mechanical vibration has attracted interest because it can modulate both movement and movement perception without rigid linkages or surface electrodes, suggesting a lightweight, patient-friendly alternative [9].

Vibration applied to muscle or tendon elicits the tonic vibration reflex (TVR)—a spinally mediated response in which high-frequency stimulation (~20–300 Hz) excites Ia afferents and produces involuntary, sustained contraction [10]. Reflex magnitude increases with both stimulation frequency and displacement amplitude; for instance, raising vibration amplitude on the masseter from 0.4 mm to 1.6 mm markedly elevates EMG activity [11]. Because the reflex loop is confined to the spinal cord, the resulting force is generated without cortical input—an important advantage for patients who lack reliable voluntary command [10]. TVR amplitude is further modulated by muscle state, stimulus parameters, and inter-subject variability [10][12]. Its ability to produce joint torque without external actuation has already inspired applications in motion augmentation, prosthetic control, and tremor

suppression [13]-[17], and serves as the neuromechanical foundation for the present vibration-based rehabilitation study.

Previous studies have shown that vibration-evoked TVR can generate single-joint motion in the upper limb, underscoring their promise for neurorehabilitation [9]. The present work extends vibration-based stimulation to multi-degree-of-freedom (multi-DOF) control and examines how joint-specific frequency combinations influence reflex-driven motor output. In this study, mechanical vibration is applied to four muscles (the pectoralis major, posterior deltoid, biceps brachii, and triceps brachii) to elicit coordinated shoulder horizontal adduction/abduction and elbow flexion/extension. By systematically varying the stimulation frequencies delivered to each muscle pair, the study quantifies frequency-dependent changes in activation strength and inter-joint coordination, providing new insight into the tuning characteristics of TVR in a multi-joint context and offering guidance for the design of adaptive, vibration-based rehabilitation systems.

2. PROPOSED METHOD

Figure 1 outlines the conceptual foundation of the proposed vibration-based rehabilitation strategy. The long-term objective is to convert cortical motor intention directly into joint torque by exploiting the TVR. High-frequency stimulation of selected muscles engages spinal reflex pathways, generating involuntary force that drives limb motion without external actuators. Because practical rehabilitation tasks demand coordinated, multi-DOF actions, the present work investigates how joint-specific adjustments of vibration

frequency can modulate the overall arm response, rather than relying on a single, uniform stimulus.

The upper-limb synergy chosen for investigation combines shoulder horizontal adduction/abduction with elbow flexion/extension, a pairing representative of functional reaching. Four muscles act as stimulation targets: the pectoralis major and posterior deltoid govern the shoulder component, whereas the biceps brachii and triceps brachii control the elbow. Vibrators are mounted directly over each muscle belly, allowing the frequency delivered to the shoulder pair to be set independently from that applied to the elbow pair. By maintaining constant burst duration, preload force, and vibration amplitude, any change in kinematic or perceptual outcome can be attributed to frequency manipulation alone.

The method therefore evaluates a matrix of heterogeneous frequency conditions—including matched and mismatched pairings—to quantify their effects on joint-specific activation magnitude, inter-joint coordination, and the strength of the induced kinesthetic percept. Insights gained from this frequency-tuning paradigm are expected to inform the development of adaptive, intention-aligned vibration interfaces capable of delivering patient-specific multi-DOF rehabilitation without external mechanical actuation.

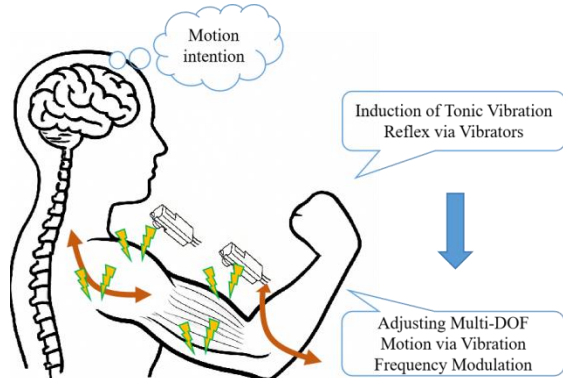


Fig.1 Conceptual framework of vibration-induced Multi-DOF movement via TVR.

3. EXPERIMENTS

3.1 Experimental setup

The experiment sought (i) to confirm that mechanical vibration alone can generate multi-DOF movement through tonic vibration reflexes, and (ii) to determine how joint-specific modulation of TVR intensity alters overall upper-limb kinematics.

The study was conducted with three right-handed, neurologically intact adults (mean age = 27.4 ± 3.4 yr; two males, one female) who gave written informed consent; the protocol was approved by the Kyushu University School of Engineering ethics committee (H28-04). Mechanical vibration was produced by a custom actuator driven by a carbon-brush DC motor (Mabuchi RS-380PH) equipped with a 1.5 mm eccentric mass, yielding a peak-to-peak displacement of 3.0 mm. Motor speed and thus vibration

frequency, adjustable from 20 Hz to 160 Hz, was monitored by an incremental encoder (Nidec Copal RE12D-300-201) and stabilised in real time through an on-board proportional–derivative loop implemented on an Arduino Mega. The vibrator was pre-loaded against the skin with a 3 N normal force verified by a FlexiForce A205-1 thin-film sensor. Upper-limb kinematics were captured with a dual-camera OptiTrack V120-Duo system; reflective markers placed on the shoulder, elbow, and wrist provided sub-millimetre, three-dimensional trajectories from which joint angles and resultant displacements were computed for subsequent TVR- and KI-related analyses.

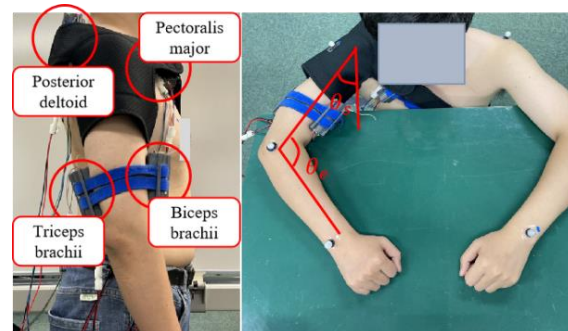


Fig.2 Experimental setup.

Figure 2 illustrates the experimental setup used to deliver joint-specific vibration and record two-degree-of-freedom kinematics. In the left panel, four miniature vibrators (20–150 Hz range) are secured directly over the target muscle bellies with low-stretch straps: the posterior deltoid (upper-posterior shoulder), pectoralis major (clavicular portion), biceps brachii (mid-anterior upper arm), and triceps brachii (mid-posterior upper arm). These two agonist-antagonist pairs generate shoulder horizontal adduction/abduction and elbow flexion/extension, respectively, allowing independent frequency assignment at each joint.

The right panel shows the participant's standardised posture and the reflective-marker configuration used for motion capture. Markers placed on the acromion, lateral epicondyle, and radial styloid define two planar joint angles: θ_s (shoulder horizontal adduction/abduction) and θ_e (elbow flexion/extension). A marker at C7 references trunk position, ensuring limb movement is measured relative to the torso. The right arm, positioned with the elbow near 90° and the forearm pronated, serves as the stimulated limb for all trials, while the left arm remains relaxed on the tabletop. This arrangement provides accurate, sub-millimetre tracking of multi-DOF trajectories and isolates the mechanical effects of vibration-evoked tonic vibration reflexes on upper-limb coordination. The angles of shoulder horizontal adduction and elbow extension are set to positive.

3.2 Experimental Procedure

In the experiment, which examined motion induction via the TVR, vibration stimuli were applied in alternating muscle pairs to elicit passive, two-DOF upper-limb movements without voluntary activation.

To evoke reciprocal motion, two specific muscle pairings were stimulated: (1) simultaneous vibration of the pectoralis major and biceps brachii, intended to produce shoulder horizontal adduction coupled with elbow flexion, and (2) stimulation of the posterior deltoid and triceps brachii, eliciting the opposing pattern—shoulder horizontal abduction with elbow extension. When effective, sequential activation of these two muscle groups produces a closed-loop, alternating joint movement pattern.

Each trial consisted of a repeated sequence. Participants were positioned in a standardized seated posture and asked to remain entirely passive. A 8-second burst of vibration was first applied to the posterior deltoid and triceps pair on the right arm, followed immediately by a 8-second burst to the pectoralis major and biceps. This two-phase cycle was then repeated once, resulting in a total trial duration of 32 seconds. Six frequency conditions were tested (as shown in Table 1). In the first three, vibration to the pectoralis major/biceps pair was fixed at 90 Hz while posterior deltoid/triceps pair was stimulated at 60, 90, or 120 Hz. In the remaining three, the posterior deltoid/triceps pair was fixed at 90 Hz and the pectoralis major/biceps pair was varied across the same three frequencies. All other stimulus parameters were held constant.

Table 1 Vibration-frequencies for Experiments

Simulation Conditions	Frequencies applied	
	Fixed muscle pair (frequency)	Variable muscle pair (frequency)
Block A, Trial 1	Pectoralis major/biceps pair (90Hz)	Posterior deltoid/triceps pair (60Hz)
Block A, Trial 2	Pectoralis major/biceps pair (90Hz)	Posterior deltoid/triceps pair (90Hz)
Block A, Trial 3	Pectoralis major/biceps pair (90Hz)	Posterior deltoid/triceps pair (120Hz)
Block B, Trial 4	Posterior deltoid/triceps pair (90Hz)	Pectoralis major/biceps pair (60Hz)
Block B, Trial 5	Posterior deltoid/triceps pair (90Hz)	Pectoralis major/biceps pair (90Hz)
Block B, Trial 6	Posterior deltoid/triceps pair (90Hz)	Pectoralis major/biceps pair (120Hz)

4. RESULTS

Figure 3 compares elbow (top) and shoulder (bottom) angle-change trajectories for Trials 1–3, in which the posterior-deltoid/triceps pair was held at 90 Hz while the pectoralis-major/biceps pair was driven at 60, 90, and 120 Hz, respectively. Each trial consists of two 8 s vibration bursts (shaded by the red dashed markers): first the variable-frequency burst (0–8s, 16–24s) followed by the fixed-frequency burst (8–16s, 24–32s).

During the fixed-frequency segments (second burst of each cycle), the three traces converge almost perfectly—angular slopes for both θ_e and θ_s are nearly identical—confirming that a common 90 Hz stimulus delivers reproducible reflex-driven motion irrespective of the preceding condition. The angles of shoulder

horizontal adduction and elbow extension are set to positive.

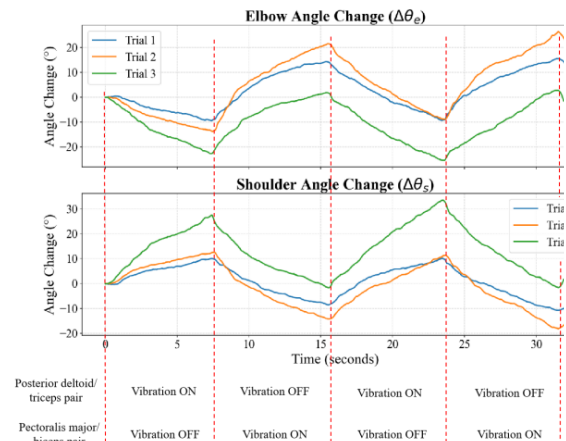


Fig.3 Time-series of elbow and shoulder angle changes for Trials 1–3 of subject 1.

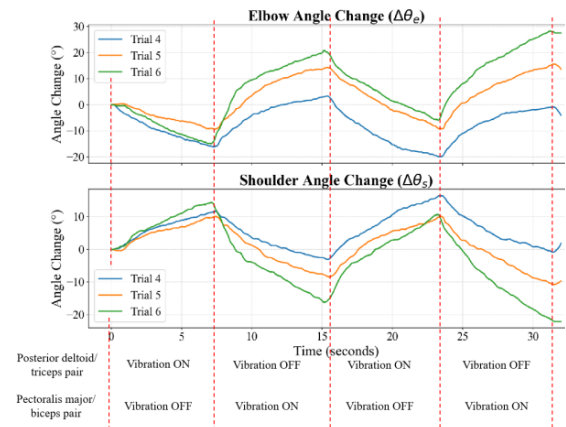


Fig.4 Time-series of elbow and shoulder angle changes for Trials 4–6 of subject 1.

In contrast, the variable-frequency segments (first burst of each cycle) show pronounced divergence. At 60 Hz (Trial 1, blue), both joints accelerate more slowly, yielding shallower trajectories; at 120 Hz (Trial 3, green) they accelerate steeply, producing faster and larger displacements; 90 Hz (Trial 2, orange) lies in-between. The clear separation of slopes indicates that TVR-induced rate of angle change is frequency-dependent and that selective frequency modulation at one muscle pair reshapes the overall multi-DOF movement profile while leaving the subsequent common-frequency response unchanged.

Figure 4 depicts the joint-angle trajectories for Trials 4–6, in which the pectoralis-major/biceps pair was held at 90 Hz while the posterior-deltoid/triceps pair received 60, 90, or 120 Hz stimulation. Each trace comprises four 8-s vibration epochs, separated by the red dashed lines: the first and third epochs apply the variable-frequency burst, whereas the second and fourth epochs repeat the common 90 Hz burst. During the common-frequency epochs (8–16s and 24–32s) the three curves nearly overlap, confirming that a uniform 90 Hz stimulus evokes reproducible elbow- and shoulder-angle

responses irrespective of the preceding condition. In contrast, the variable-frequency epochs (0–8s and 16–24s) diverge markedly. When the posterior-deltoid/triceps pair is driven at 60 Hz (Trial 4, blue) both joints accelerate more slowly, producing the shallowest trajectories; at 120 Hz (Trial 6, green) they accelerate rapidly and reach the largest displacements, with 90 Hz (Trial 5, orange) lying between the two extremes. The differential is most pronounced in the shoulder traces, indicating that frequency tuning at the proximal extensor–flexor pair reshapes global limb coordination while exerting its greatest effect on the joint directly innervated by the modulated muscles.

Table 2 The average elbow angular velocity response of Experiments

Trial	The average elbow angular velocity response (°/s)					
	Subject 1		Subject 2		Subject 3	
	Fixed pair	Var. pair	Fixed pair	Var. pair	Fixed pair	Var. pair
1	2.4	1.2	1.9	1.1	1.8	0.9
2	2.0	1.4	1.8	1.5	2.0	1.1
3	2.2	2.4	1.8	2.0	1.7	1.8
4	2.3	1.9	2.3	1.4	2.2	1.1
5	2.1	2.4	2.1	2.3	1.8	1.4
6	2.4	3.2	2.0	2.5	1.7	2.3

Table 3 The average shoulder angular velocity response of Experiments

Trial	The average shoulder angular velocity response (°/s)					
	Subject 1		Subject 2		Subject 3	
	Fixed pair	Var. pair	Fixed pair	Var. pair	Fixed pair	Var. pair
1	1.4	0.8	1.2	0.8	1.5	0.7
2	1.5	1.2	1.0	0.9	1.2	1.0
3	1.4	2.0	1.1	1.3	1.3	1.4
4	1.6	1.2	1.2	1.1	1.4	0.9
5	1.3	1.3	1.4	1.1	1.2	1.1
6	1.5	2.2	1.4	1.6	1.3	1.8

Tables 2 and 3 summarise the mean angular-velocity responses of the elbow and shoulder, respectively, for three participants across the six vibration trials. In each trial one muscle pair was stimulated at a fixed 90 Hz, whereas the antagonist pair received a variable frequency of 60, 90, or 120 Hz. Two systematic effects emerge. First, the segment driven at the variable frequency exhibits a monotonic, frequency-dependent change in velocity: when the posterior-deltoid/triceps pair served as the variable group (Trials 1–3), elevating its frequency from 60 Hz to 120 Hz increased elbow velocity from approximately 1 °/s to more than 3 deg s⁻¹ and shoulder velocity from roughly 0.8 °/s to over 2 °/s; an equivalent trend appears in Trials 4–6 when the pectoralis-major/biceps pair is varied. Second, the fixed pair remains remarkably stable; across all six trials its

mean velocity fluctuates by less than 0.3 °/s for every subject, indicating that a constant 90 Hz stimulus evokes a reproducible tonic-reflex response independent of frequency changes at the antagonist joint. Collectively, these data confirm that TVR-driven multi-DOF motion can be selectively scaled through local frequency tuning while preserving a reliable baseline in the non-modulated musculature.

5. CONCLUSION

This study demonstrated that multi-DOF upper-limb motion can be regulated exclusively through TVR stimulation when different muscle pairs are driven at joint-specific frequencies. Holding one agonist–antagonist pair at a constant 90 Hz produced a highly repeatable baseline response, whereas sweeping the frequency of the opposing pair from 60 Hz to 120 Hz systematically scaled angular-velocity magnitude and altered shoulder–elbow coordination. Across all participants, the variable-frequency muscle pair exhibited a monotonic increase in mean angular velocity, while the fixed-frequency pair remained effectively unchanged, confirming that local frequency tuning affords selective, joint-level control without cross-interference. These results establish frequency-dependent TVR modulation as a lightweight, actuator-free means of shaping multi-DOF arm kinematics and provide quantitative design guidelines for adaptive vibration interfaces in neurorehabilitation.

REFERENCES

- [1] V. L. Feigin, M. Brainin, B. Norrving, S. Martins, R. L. Sacco, W. Hacke et al., “World Stroke Organization (WSO): global stroke fact sheet 2022,” *Int. J. Stroke*, vol. 17, no. 1, pp. 18–29, Jan. 2022.
- [2] A. N. Malik, H. Tariq, A. Afridi, and F. Azam Rathore, “Technological advancements in stroke rehabilitation,” *J. Pak. Med. Assoc.*, vol. 72, no. 8, pp. 1672–1674, 2022.
- [3] S. G. Rozevink, J. M. Hijmans, K. A. Horstink, and C. K. van der Sluis, “Effectiveness of task-specific training using assistive devices and usual care on upper-limb performance after stroke: a systematic review and meta-analysis,” *Disabil. Rehabil. Assist. Technol.*, vol. 18, no. 7, pp. 1245–1258, 2023.
- [4] A. Demofonti, G. Carpino, L. Zollo, and M. J. Johnson, “Affordable robotics for upper-limb stroke rehabilitation in developing countries: a systematic review,” *IEEE Trans. Med. Robot. Bionics*, vol. 3, no. 1, pp. 11–20, 2021.
- [5] S. Straudi et al., “Effectiveness of robot-assisted arm therapy in stroke rehabilitation: An overview of systematic reviews,” *NeuroRehabilitation*, vol. 51, no. 4, pp. 559–576, 2022.
- [6] K. Kiguchi, R. Esaki, T. Tsuruta, K. Watanabe, and T. Fukuda, “An exoskeleton system for elbow joint motion rehabilitation,” in *Proc. IEEE/ASME Int. Conf. Adv. Intell. Mechatronics (AIM)*, vol. 2, Jul. 2003, pp. 1228–1233.

- [7] G. Ye, E. P. Grabke, M. Pakosh, J. C. Furlan, and K. Masani, "Clinical benefits and system design of FES-rowing exercise for rehabilitation of individuals with spinal cord injury: a systematic review," *Arch. Phys. Med. Rehabil.*, vol. 102, no. 8, pp. 1595–1605, Aug. 2021.
- [8] E. González-Graniel et al., "Sensing and control strategies used in FES systems aimed at assistance and rehabilitation of foot drop: a systematic literature review," *J. Pers. Med.*, vol. 14, no. 8, Art. no. 874, 2024.
- [9] K. Kiguchi and K. Maemura, "Simultaneous control of tonic vibration reflex and kinesthetic illusion for elbow-joint motion toward novel robotic rehabilitation," in *Proc. 43rd Annu. Int. Conf. IEEE Eng. Med. Biol. Soc. (EMBC)*, Nov. 2021, pp. 4773–4776.
- [10] G. Eklund and K. E. Hagbarth, "Normal variability of tonic vibration reflexes in man," *Exp. Neurol.*, vol. 16, no. 1, pp. 80–92, Sep. 1966.
- [11] J.P. Roll, J.P. Vedel, E. Ribot, "Alteration of proprioceptive messages induced by tendon vibration in man: a microneurographic study," *Exp. Brain Res.*, vol. 76, no. 1, pp. 213–222, 1989.
- [12] W. Liu, Y. Chen, K. Kiguchi, and M. Svinin, "Fundamental study on the influence of muscle fatigue on tonic vibration reflex," in *Proc. IEEE/SICE Int. Symp. Syst. Integr. (SII)*, Jan. 2025, pp. 464–468.
- [13] M. Abe, S. Nishikawa, and K. Kiguchi, "Generation of hand reaching motion illusion using vibration stimulation," in *Proc. IEEE Int. Conf. Syst., Man, Cybern. (SMC)*, Oct. 2023, pp. 1641–1646.
- [14] K. Honda, K. Kiguchi, "Control of human motion change based on vibration stimulation for upper-limb perception-assist," *IEEE Access*, vol. 8, pp. 22697–22708, 2020.
- [15] P. G. S. Alva, A. Boesendorfer, O. C. Aszmann, J. Ibáñez, and D. Farina, "Excitation of natural spinal reflex loops in the sensory-motor control of hand prostheses," *Sci Robot*, vol. 29, no. 9, 2024.
- [16] W. Liu, T. Kai, K. Kiguchi, "Tremor suppression with mechanical vibration stimulation," *IEEE Access*, vol. 8, pp. 226199–226212, 2020.
- [17] K. Kiguchi, T. Kai, and W. Liu, "A fundamental study on tonic vibration reflex in forearm pronation/supination to suppress essential tremor movements," in *Proc. IEEE Int. Conf. Syst., Man, Cybern. (SMC)*, Oct. 2020, pp. 2668–2673.